

---

## Design and analysis of multi-band circle shape MIMO antenna using defected ground structure to reduce mutual coupling

---

**K. Vasu Babu\***

Department of ECE,  
Vasireddy Venkatadri Institute of Technology,  
A.P., India  
Email: vasubabuece@gmail.com

\*Corresponding author

**B. Anuradha**

Department of ECE,  
SV University,  
Tirupati, A.P., India  
Email: anubhuma@yahoo.com

**Abstract:** In the present paper, a multi-band circle shape MIMO radiator with and without dumbbell-shaped parasitic element for all wireless applications is proposed. The proposed antenna comprises MIMO circular shape radiating patch with U-shaped inverted slot and pair of rectangular slits. By adjusting U-shaped inverted slot, a pair of rectangular slits and neutralisation line we obtain distinct resonance frequencies centred at 3.5, 5.3, 7.0 and 8.8 GHz. The VSWR results are centred on  $\leq 2$  at these resonant frequencies. The far field values obtained at a wide operational bandwidth, the simulated results represent that the multi-band antenna can cover sufficient bandwidth for entire frequency bands. The multi-band antenna also shows a radiation pattern of an omni directional with an acceptable average peak gains at the resonant frequencies are 5.238 dBi, 7.044 dBi, 6.763 dBi and 7.852 dBi of LTE/WLAN bands, WiMAX band, and ITU and satellite band system applications.

**Keywords:** WiMAX; WLAN; MIMO patch antenna; neutralisation line; U-shaped slot.

**Reference** to this paper should be made as follows: Babu, K.V. and Anuradha, B. (2019) ‘Design and analysis of multi-band circle shape MIMO antenna using defected ground structure to reduce mutual coupling’, *Int. J. Ultra Wideband Communications and Systems*, Vol. 4, No. 1, pp.32–40.

**Biographical notes:** K. Vasu Babu is working as an Assistant Professor in E.C.E Department at the Vasireddy Venkatadri Institute of Technology, Guntur, A.P., and India. He is currently pursuing his PhD degree from the SV University, Tirupati, India. His areas of interest include design of microstrip and dielectric resonator antennas for MIMO applications. He published more than 20 research papers in referred journals.

B. Anuradha is working as a Professor and the HoD in E.C.E Department at the SVU College of Engineering, Tirupati, India. She obtained her PhD degree from the SV University, Tirupati, India in 2008. Her areas of interest include design of microstrip and dielectric resonator antennas for MIMO applications and biomedical engineering. She published more than 110 research papers in referred journals. She is currently a reviewer for many reputed journals.

---

### 1 Introduction

In order to specify the suitable shape and minimum size of the conductor lines can be optimised by frequency response of different circuits and microwave component. The metal sheet like copper is used to make up of backside of the ground plane components and does not distribute any freedom in the phase design. There is another way to improve the microwave component characteristics depend on the microstrip lines and CPW is defected ground structure (DGS) (Garg et al., 2013). The technique is

defined as an etching or any modification inside the area of ground plane modify its consistency is generally introduce to be a defect. For proper coupling to the antenna or microstrip line DGS is placed beneath a microstrip line or antenna. By using this type of technique effects the change in the current distribution and input impedance of the antenna and also reduces the size of the antenna with respect to size and resonate frequency. The different approaches of designs like dual-band, tri-band and multi-band antennas for WiMAX/WLAN and C-band operation reported (Park et al., 2001; Abdel-Rahman et al.,

2004; Abidin et al., 2010; Bait-Suwailam et al., 2010; Sung et al., 2003; Sung and Kim, 2005; Chiu et al., 2007; Mahmoudian and Rashed-Mohassel, 2008; Zhu et al., 2009; Zulkifli et al., 2010, 2008; Salehi and Tavakoli, 2006; Guha et al., 2005; Yu and Zhang, 2003; Islam and Alam, 2013; Farsi et al., 2012; Alsath et al., 2013; Suwailam et al., 2010; Shafique et al., 2015; Yang et al., 2012; Chaimool et al., 2012; Xiao et al., 2011; Kumar and Guha, 2014, 2012; Khandelwal et al., 2014a, 2014b). In Park et al. (2001),  $65 \times 65 \text{ mm}^2$  size of antenna design with the LPF using microstrip DGS. A single-negative magnetic metamaterial is used to reduction of electromagnetic coupling for MIMO applications with a resonant frequency of 1.15 GHz with dimensions of  $1.25\lambda \times 1.25\lambda$  (Bait-Suwailam et al., 2010). A  $52 \times 52 \text{ mm}^2$  CPW fed antenna with operating band of 3.5 to 3.64, 4.46 to 4.52 and 5.8 to 6.2 GHz three resonant frequencies at the entire band using the technique of DGS for a microstrip patch antenna reduced the harmonics was proposed in Sung et al. (2003). Reduction of mutual coupling between closely-packed antenna elements with centre to centre distance between the two patches was  $0.116\lambda_0$  was proposed in Chiu et al. (2007). The size of the antenna was  $68 \times 50 \text{ mm}^2$  while the resonant frequency of operation was 4.17 GHz. In Zulkifli et al. (2010), a dumbbell shape defect ground structure is inserted between the patches to reduce isolation for multi-band microstrip

antenna array. The overall dimensions of the antenna were  $78.26 \times 78.26 \text{ mm}^2$ . In Salehi and Tavakoli (2006), produced a resonance near 6.0 GHz using the concept of DGS is placed between the patches for antenna array design of low mutual coupling observed. Hexagonal DGS is considered for microstrip fed monopole with enhancing the radiation properties for triangular microstrip patch radiator reduced the isolation compared to without DGS with overall dimensions of  $130 \times 105 \text{ mm}^2$  in Zulkifli et al. (2008). The improvement in the isolation of 4 dB for the entire band of frequency range 2.58 to 2.62 GHz inserted DGS between the two patches. A  $74.7 \times 74.7 \text{ mm}^2$  microstrip antenna having compact structure of EBG reduced mutual coupling was presented (Islam and Alam, 2013). The compact EBG structure placed between the rectangular patch which is resonating at a frequency of 2.4 GHZ operated in the WLAN application. In Alsath et al. (2013), the implementation of one of the technique is slotted meander line resonators for microstrip array to enhancing the isolation between the patches was presented. A low frequency representation is required for achieving the isolation at 4.8 GHZ with edge to edge spacing between the patches is  $0.11\lambda_0$  for overall dimensions of  $54 \times 45 \text{ mm}^2$ . Table 1 represents the comparison of different techniques with their geometries and corresponding parameters.

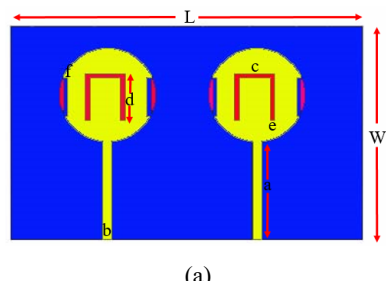
**Table 1** Antenna sizes compared with present circular shape antenna design

References	Antenna size (mm <sup>2</sup> )	Total area occupied (mm <sup>2</sup> )	S <sub>11</sub> (dB)/return loss	S <sub>12</sub> (dB)/mutual coupling	f <sub>L</sub> -f <sub>H</sub> (GHz)	Resonant frequency (GHz)
Park et al. (2001)	65 × 65	4,225	-35	-45	7.0–7.4	7.2
Bait-Suwailam et al. (2010)	120 × 110	13,200	-48	-18	1.0–1.2	1.15
Sung et al. (2003)	52 × 52	2,704	-12 -18 -11	-25 -35 -38	3.5–3.64 4.46–4.52 5.8–6.2	3.62 4.5 6
Chiu et al. (2007)	68 × 50	3,400	-26	-19.7	4.10–4.18	4.17
Zhu et al. (2009)	78.26 × 78.26	6,124.62	-18	-65	7.4–7.8	7.5
Zulkifli et al. (2010)	140 × 100	14,000	-22 -24 -20	-32 -52 -40	2.1–2.4 5.8–6.2 5.2–5.6	2.3 3.3 5.8
Salehi and Tavakoli (2006)	80 × 60	4,800	-22	-27.91	5.8–6.2	6
Zulkifli et al. (2008)	130 × 105	13,650	-43.22	-37	2.58–2.62	2.61
Islam and Alam (2013)	74.7 × 37.35	2,790.045	-22	-40	2.2–2.6	2.4
Alsath et al. (2013)	54 × 45	2,430	-18	-30	4.2–5.2	4.8
Suwailam et al. (2010)	60 × 80	4,800	-32	-26	4.1–5.1	5
Shafique et al. (2015)	60 × 70	4,200	-20.7	-37.1	3.5–3.9	3.7
Yang et al. (2012)	41 × 50.7	2,078.7	-25	-29	3.1–3.4	3.2
Chaimool et al. (2012)	110 × 110	12,100	-18 -30	-25 -35	2.4–2.484 2.3–2.5	2.42 2.4
Xiao et al. (2011)	76.4 × 91	6,952.4	-35	-50	3.0–4.0	3.5
Kumar and Guha (2014)	60 × 60	3,600	-30	-38	10.1–10.4	10.2
Kumar and Guha (2012)	50 × 35	1,750	-26	-31	2.0–2.5	2.3
Proposed system (without DGS)	50 × 40	2,000	-17 -19 -33 -35	-30 -28 -35 -32	3.3–3.6 5.0–5.7 6.8–7.3 8.5–9.0	3.5 5.3 7.0 8.8
Proposed system (with DGS)	50 × 40	2,000	-19 -22 -55 -29	-40 -32 -45 -40	3.3–3.6 5.0–5.7 6.8–7.3 8.5–9.0	3.5 5.3 7.0 8.8

## 2 Circular shape patch design

The circular shape design antenna having geometry of  $50 \times 40 \text{ mm}^2$  depicted in Figure 1 represents the circular shape MIMO antenna including ground plane and substrate. The MIMO circular antenna has two patches and they are mirrored to each other, a single patch leads to a symmetrical dimension to both axes. The circular patch has U-shaped inverted slot, with a rectangular slit on both sides. The top radius of the patch is 19. The substrate is FR-4 lossy whereas for ground, patch, slots and strip we use copper. The outer patch has  $L \times W$  dimensions. The remaining dimensions can be shown in Table 2. The material consideration is also important in the design part of antenna.

**Figure 1** Design of circular MIMO shape antenna, (a) circular shape antenna (b) fabricated antenna (see online version for colours)



(a)



(b)

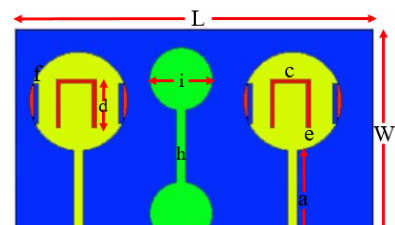
**Table 2** Dimensions of the circle shape MIMO antenna design with and without DGS structure

Design parameters	<i>L</i>	<i>W</i>	<i>a</i>	<i>b</i>	<i>c</i>	<i>d</i>	<i>e</i>	<i>f</i>	<i>g</i>	<i>h</i>	<i>i</i>	$\epsilon_r$
Value (mm)	50	40	24	2	3	5	2	2	10	3	10	4.5

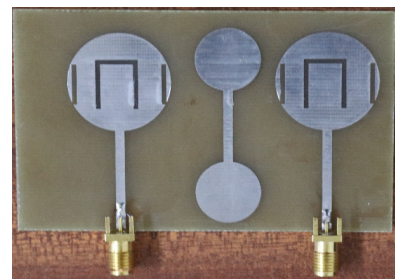
Figure 2 shows the design geometry of circular shape MIMO antenna with dumbbell-shape parasitic structure. It resembles Figure 1, there will be an extra adding of a strip of 3 mm and circle of radius 10 mm consist a rectangular slot with circular head in between the two circular patches. The material used for designing of this type of antenna is copper. In a microwave circuits, DGS is defined as a small geometrical slots embedded into the ground plane. A structure having a single defect in a unit cell or a number of periodic and aperiodic defects configurations. For planar microwave circuits the periodic and/or aperiodic defects etched on the ground plane are called DGS. Previously PBG, EBG and neutralisation technique have been reported with irregular ground planes.

Table 3 signifies that contrast of EBG, PBG and DGS with different parameters. Planar microwave circuits using periodic DGSs have drawn the attraction of the microwave researchers. The method used to get larger slow wave rate with miniaturisation is obtained by periodic structures. When we consider a finite spacing, repetition of particular defect occurred is referred to as periodic structure. The cascaded resonant cells effect the ground plane depends on total periods return loss and improvement in the bandwidth. Figure 3 describes the conventional analysis and design methods in DGSs.

**Figure 2** Design of circular shape MIMO with dumbbell-shape parasitic, (a) circular shape antenna with DGS (b) fabricated antenna with DGS (see online version for colours)



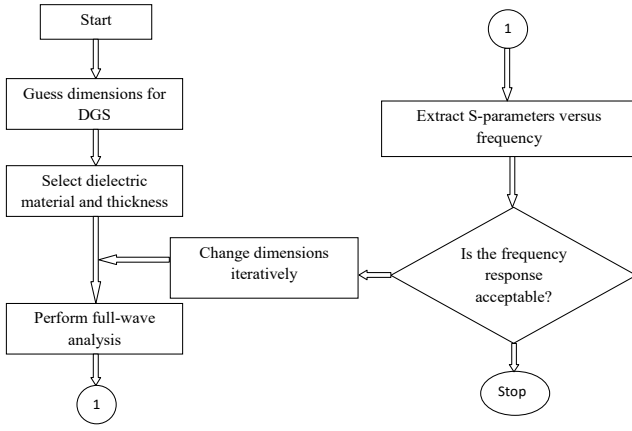
(a)



(b)

**Table 3** Comparison of PBG, EBG and DGS

	PBG	EBG	DGS
Definition	An electromagnetic waves which have the ability to control propagation of waves consists periodic structures etched on the ground plane called PBG	A structure which have compact in size realised by periodic structure similar to that of PBG is called EBG.	In microwave circuits, at the ground plane embedded one or limited geometrical slots is called DGS.
Geometry	A periodic etched structure	Periodic etched structure	One or few etched structures
Parameter extraction	Very difficult	Very difficult	Relatively simple
Size	Large	Smaller than PBG and larger than DGS	Much more compact than PBG and EBG
Fabrication	Difficult	Difficult	Easy

**Figure 3** Flowchart of rectangular slot with circular head DGS

### 3 Multiple input multiple output

The different types of parameters that describe the MIMO operation can be evaluated by mathematical expression. Total active reflection coefficient is evaluated by Chae et al. (2007).

$$TARC = \sqrt{|S_{11} + S_{12}e^{j\theta}|^2 + |S_{21} + S_{22}e^{j\theta}|^2} / \sqrt{2} \quad (1)$$

where  $\theta$  describes the value between 0 to  $2\pi$ .

The second type of parameter correlation coefficient is evaluated by Blanch et al. (2003).

$$\rho \approx |\rho_{cij}|^2 \quad (2)$$

The correlation coefficient ( $\rho$ ) represented by the scattering parameters determined as follows by Blanch et al. (2003) indicates that the correlation coefficient ( $\rho$ ) of an array antenna shows the effect of various propagation paths of radio frequency signals that reach the radiator elements. These elements are deliberated in to the two different ways of approach one by scattering parameters and the other by far-field radiation pattern.

$$\rho(i, j, N) = \frac{\left| \sum_{n=1}^N S_{i,n}^* S_{n,j} \right|^2}{\prod_{k=i,j} \left[ 1 - \sum_{n=1}^N S_{k,n}^* S_{n,k} \right]} \quad (3)$$

The channel capacity is evaluated in terms of distribution of Gaussian function and Shannon capacity is (Stutzman and Thiele, 1998; Chae et al., 2007; Blanch et al., 2003; Shin and Lee, 2003) related to in terms of information handling of a given channel capacity. The parameters like Shannon capacity ' $c$ ', channel transfer matrix ' $H$ ' is given by Stutzman and Thiele (1998)

$$C = \log_2 \left( \det \left( 1 + \frac{SNR}{M} HH' \right) \right) \quad (4)$$

By increasing the number of antenna elements theoretically the channel capacity of the MIMO system is also increases.

In order to know about the how much amount loss in the channel is evaluated the parameter capacity loss is given by Shin and Lee (2003)

$$C_{loss} = -\log_2 \det(\Psi^R) \quad (5)$$

$$\Psi^R = \begin{pmatrix} \rho_{1,1} & \cdots & \rho_{1,N} \\ \vdots & \ddots & \vdots \\ \rho_{N,1} & \cdots & \rho_{N,N} \end{pmatrix} \quad (6)$$

$$\Psi^R = \begin{pmatrix} \rho_{11} & \rho_{12} \\ \rho_{21} & \rho_{22} \end{pmatrix} \quad (7)$$

$$\rho_{ii} = 1 - (|S_{ii}|^2 + |S_{ij}|^2) \text{ and } \rho_{ii} = -(s_{ii}^* S_{ij} + s_{ij}^* S_{jj}), \quad (8)$$

for  $i, j = 1 \text{ or } 2$

where  $\Psi^R$  is the receiving antenna correlation matrix.

**Table 4** Circle shape MIMO antenna design with dumbbell-shape parasitic element in contrast to MIMO parameters at different frequencies

S. no	Frequency (GHz)	Correlation coefficient ( $\rho$ )	TARC (dB)	Channel capacity (bits/s/Hz)	Capacity loss in (bits/s/Hz)
1	3.5	0.0014	-19.63	4.097	0.57
2	5.3	0.0018	-22.87	4.085	0.46
3	7.0	0.0036	-29.45	4.027	0.32
4	8.8	0.0024	-24.37	4.069	0.43

### 4 Results analysis

Circular MIMO shape radiator with and without dumbbell-shape parasitic structures were analysed. Here simulation results describes the multi-band characteristics for both antennas operated at four distinct resonant frequencies like 3.5, 5.3, 7.0 and 8.8 GHz as indicate Figure 4 and Figure 8 for the applications of ultra wide band antennas (UWB). Figure 6 shows the comparison of return loss and mutual coupling without dumbbell-shape parasitic structure. Here we observe that from the simulation graph that the impedance bandwidth from 3.3–3.6 GHz (300 MHz), 5.0–5.7 GHz (700 MHz), 6.8–7.3 GHz (500 MHz) and 8.5–9.0 GHz (500 MHz). For circular MIMO analysis we observed that there is an improvement in terms of impedance matching is obtained perfectly for with and without dumbbell-shape parasitic structures. Figure 6 depicts that a comparison of simulated and measured S-parameters without dumbbell-shape parasitic structure. From the findings it can be observed that circular shape antenna consist with and without dumbbell-shape parasitic structure have the parameter of return losses -17 dB resonant at a frequency 3.5 GHz and -19 dB frequency at 3.5 GHz, -19 dB and -22 dB at frequency 5.3 GHz, -33 dB and -55 dB at frequency 7.0 GHz and -35 dB and -29 dB at frequency 8.8 GHz. These parameters are an improvement of  $S_{11}$  of 11.76%, 15.78%, 66.66% and 20.68%. More power is radiated because of improving in  $S_{11}$  represents the

reflection is decreased and increases in antenna efficiency. Figure 5 and Figure 9 indicate the performance analysis of proposed radiator mutual coupling for all four resonant bands for circular shaped MIMO antenna. Figure 10 shows the distinct graph of  $S_{11}$  and  $S_{12}$  with dumbbell-shape parasitic structure. Figure 11 shows the contrast of S-parameters for measured and simulated with dumbbell-shape parasitic structure. The parameter  $S_{12}$  is improved here around  $-30$  dB to  $-40$  dB at a frequency  $3.5$  GHz with applying dumbbell-shape parasitic structure between the two patches and compared with without dumbbell-shape parasitic structure. For the second resonant frequency of around  $-28$  dB to  $-32$  dB, the third resonant frequency band around  $-35$  dB to  $-45$  dB. Meanwhile, for the final band of frequency around  $-32$  dB to  $-40$  dB. Finally, Figure 10 shows all S-parameters comparison of MIMO circle shape antenna with and without dumbbell-shape parasitic structure. A substantial decrease in  $S_{12}$  (mutual coupling) entire band of UWB applications. In addition, the antenna gain, directivity, surface current distribution and the patterns of radiation of circular MIMO is also measured for both the cases for all four resonant bands. The directivity representation for with and without dumbbell-shape parasitic structure is depicted Figure 11.

**Figure 4**  $S_{11}$  against frequency without dumbbell-shape parasitic element (see online version for colours)

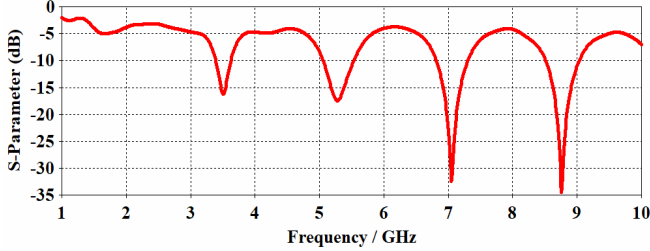


**Figure 5**  $S_{12}$  against frequency without dumbbell-shape parasitic element (see online version for colours)

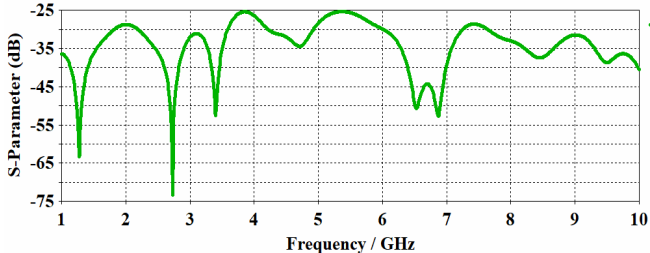


**Figure 6** Contrast of  $S_{11}$  and  $S_{12}$  without dumbbell-shape parasitic element (see online version for colours)

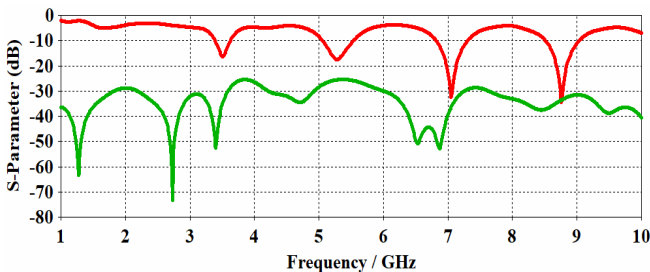


**Figure 7** Contrast measured and simulated results without dumbbell-shape parasitic element (see online version for colours)

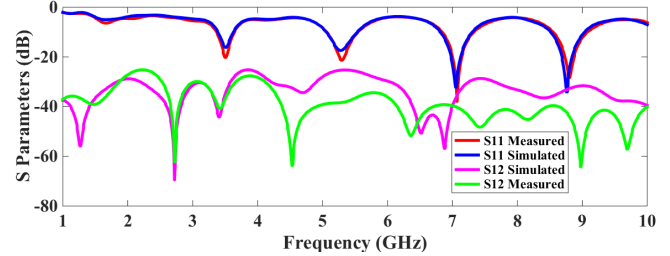


**Figure 8**  $S_{11}$  against frequency with dumbbell-shape parasitic element (see online version for colours)

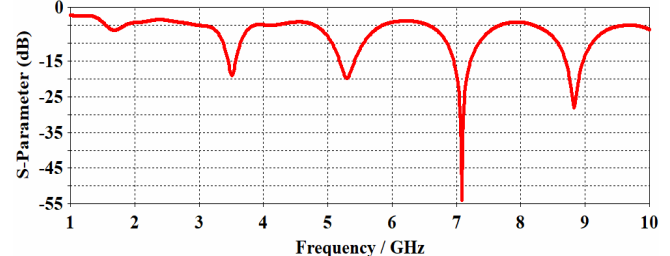


**Figure 9**  $S_{12}$  against frequency with dumbbell-shape parasitic element (see online version for colours)

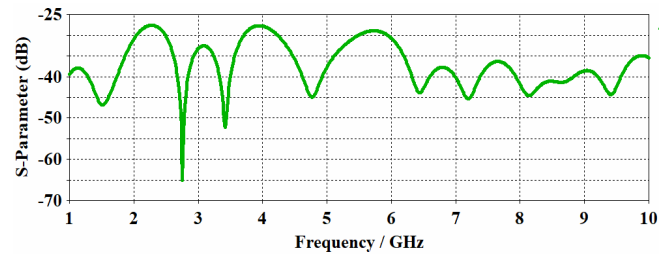


**Figure 10** Contrast of  $S_{11}$  and  $S_{12}$  without dumbbell-shape parasitic element (see online version for colours)

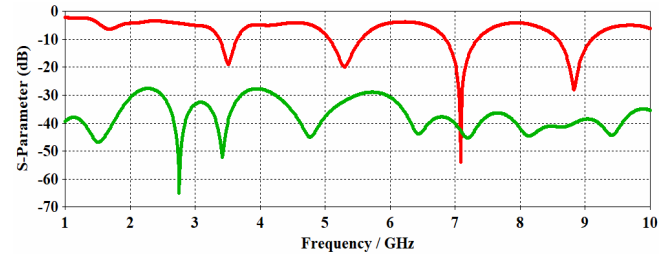


**Figure 11** Contrast of measured and simulated results with dumbbell-shape parasitic element (see online version for colours)

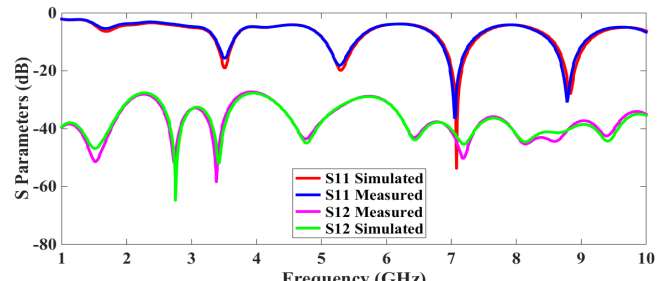


**Figure 12** The surface current distribution of circle MIMO shape radiator with a dumbbell-shaped parasitic element, (a) frequency = 3.5 GHz (b) frequency = 5.3 GHz (c) frequency = 7.0 GHz (d) frequency = 8.8 GHz (see online version for colours)

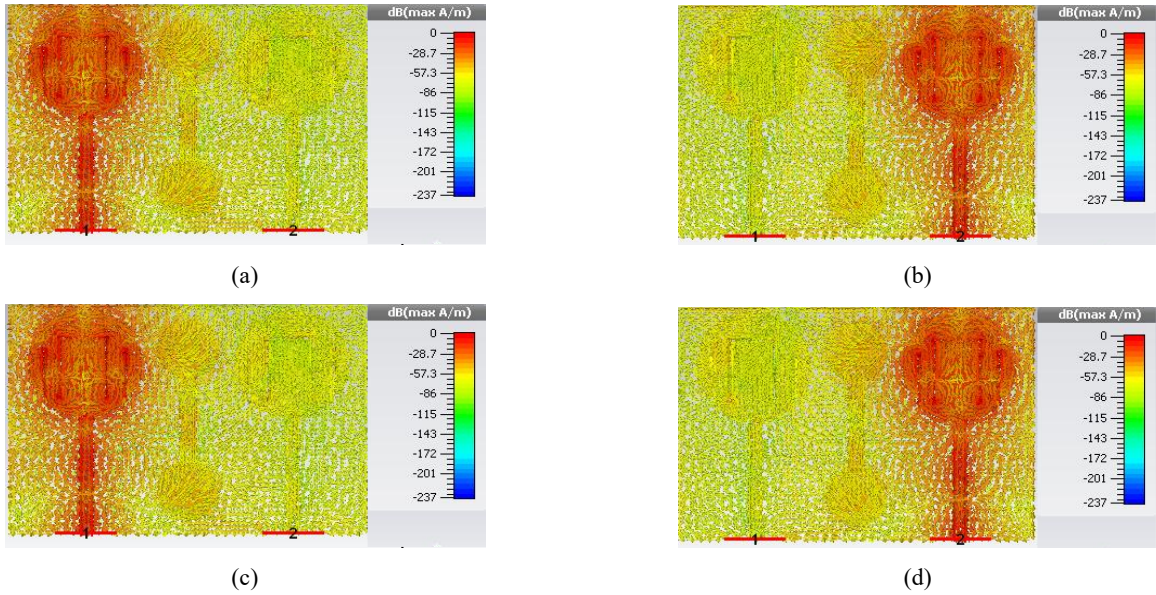


**Figure 13** The surface current distribution of circle MIMO shape radiator without a dumbbell-shaped parasitic element, (a) frequency = 3.5 GHz (b) frequency = 5.3 GHz (c) frequency = 7.0 GHz (d) frequency = 8.8 GHz (see online version for colours)

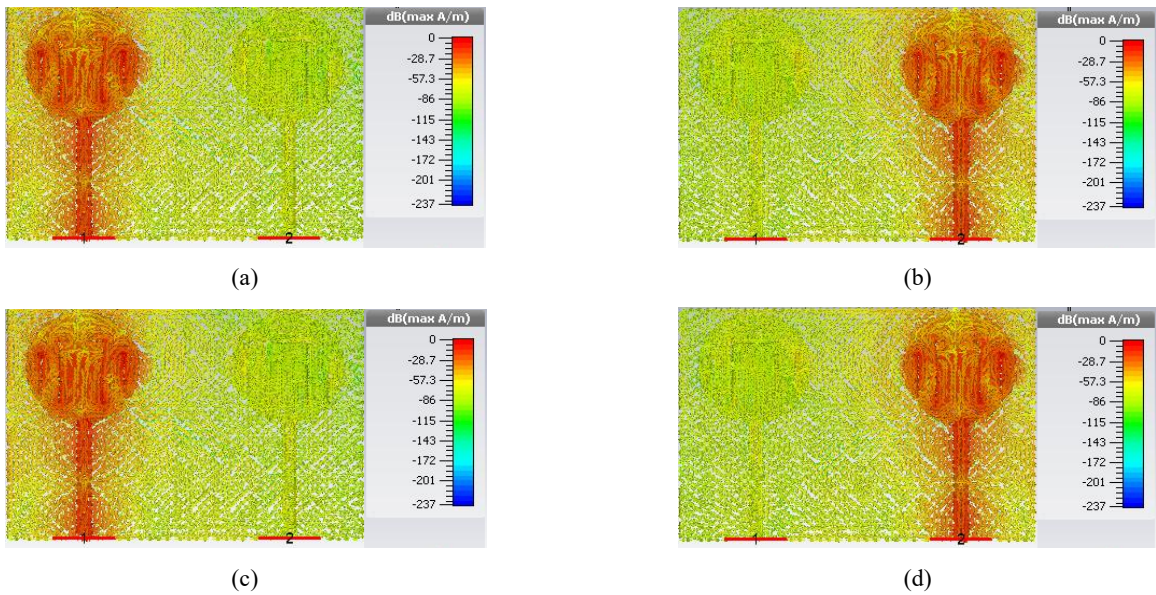
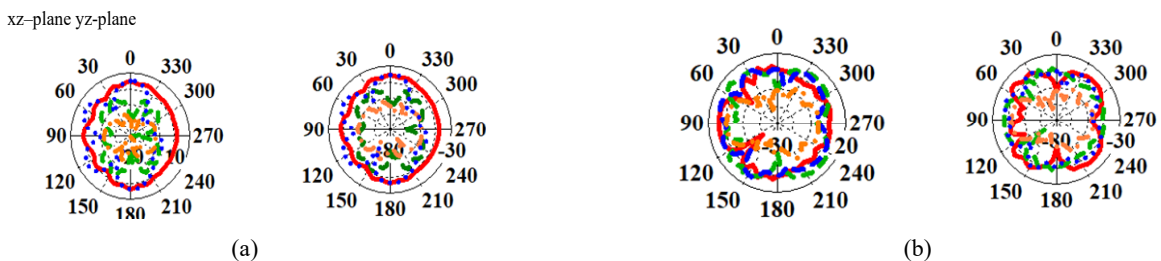
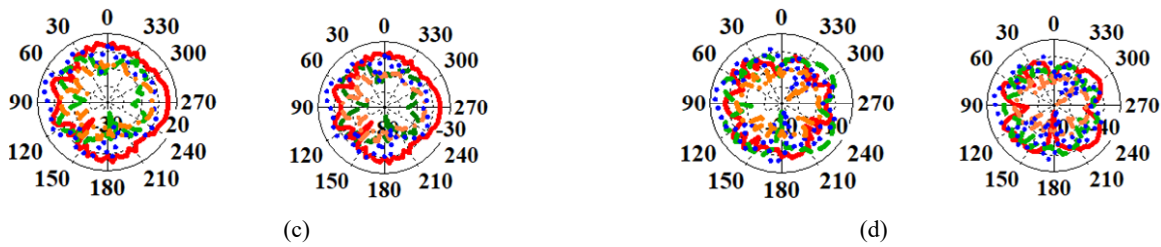


**Figure 14** Radiation pattern of circular MIMO shape without dumbbell-shape parasitic element, (a)  $f = 3.5$  GHz  
(b)  $f = 5.3$  GHz (c)  $f = 7.0$  GHz (d)  $f = 8.8$  GHz (see online version for colours)



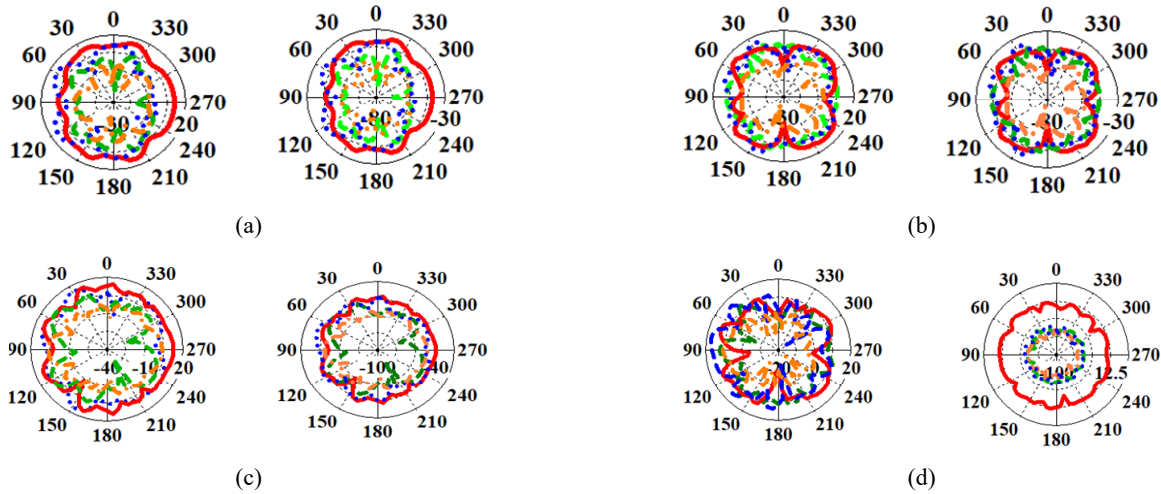
Notes: — cross polarisation simulated, — co polarisation simulated, — co polarisation measured, — cross polarisation measured.

**Figure 14** Radiation pattern of circular MIMO shape without dumbbell-shape parasitic element, (a)  $f = 3.5$  GHz (b)  $f = 5.3$  GHz (c)  $f = 7.0$  GHz (d)  $f = 8.8$  GHz (continued) (see online version for colours)



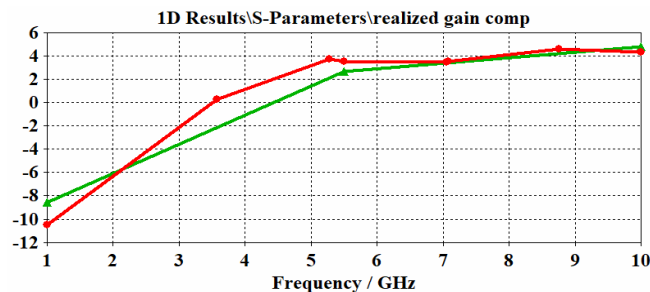
Notes: — cross polarisation simulated, — co polarisation simulated, — co polarisation measured, — cross polarisation measured.

**Figure 15** Radiation pattern of circular MIMO shape with dumbbell-shape parasitic element, (a)  $f = 3.5$  GHz (b)  $f = 5.3$  GHz (c)  $f = 7.0$  GHz (d)  $f = 8.8$  GHz (see online version for colours)



Notes: — cross polarisation simulated, — co polarisation simulated, — co polarisation measured, — cross polarisation measured.

**Figure 16** Realised gain comparison of circular MIMO shape radiator (a) with (green) and (b) without (red) dumbbell-shape parasitic element (see online version for colours)



To study the operating principle of circular shaped antenna, resonating frequencies and some antenna parameters like gain, directivity and efficiency is observed. Another one more important parameter in the design of MIMO antenna is used here to reducing the mutual coupling ( $S_{12}$ ) is observed with the help of surface current distribution are plotted with frequencies of 3.5 GHz, 5.3 GHz, 7.0 GHz and 8.8 GHz which are shown in Figure 12 and Figure 13. The surface currents distribution shows the resonant behaviour of the circle shaped structure at four distinct resonant frequencies of the entire band 1.0–10.0 GHz. From Figure 12(a), it

shows that, the main radiating patch distribution of current is strong and on the right side. Therefore, it can be understood that the 3.24–3.67 GHz WiMAX resonance mainly occurs on the middle and right side of the patch. The frequency at 5.3 GHz [Figure 12(b)] noticed that the resonance occurs due to rectangular slots at end of patch on left-hand side. The frequency at 7.0 GHz [Figure 12(c)] identified rectangular slots at the corner patch on the left-hand side and right-hand side. The fourth mode of the antenna distribution of current depicted Figure 12(d), arriving the currents on the upper and lower strip formed due to the rectangular slots on feed lines and radiating patch. Similarly from Figures 13(a)–13(d) represents the distribution of surface currents at different frequencies is observed. Finally, the distribution of current concluded that design structure can generate four bands 3.5-/5.3-/7.0-/8.8 GHz for UWB applications. For multi-band radiator analysis the E & H planes for circle MIMO shaped antenna design is done using CST Microwave Studio. Figure 14 and Figure 15 indicates the co-polarisation and cross-polarisation of simulated as well as measured results (xz-plane and yz-plane) at four frequencies for without and with dumbbell-shaped parasitic element. Finally, Figure 16 shows that the comparison of realised gain of circular

MIMO shape antenna with and without dumbbell-shape parasitic element structure.

## 5 Conclusions

In the present article, a circular radiator which consists a U-shape inverted slot and pair of rectangular slits to form planar multi-band antenna. The use of pair of rectangular slits parameters like bandwidth and resonant frequency are controlled and tuned for multi-band antennas. Due to arrangement of this type of structure formation produces an omnidirectional radiation pattern and also obtains the acceptable gain for the entire band of operation. Circular shape design radiator with and without dumbbell-shaped parasitic element shows the stable acceptable radiation pattern, easy to implement the structure and also wider bandwidth in the resonant frequency. This type of proposed MIMO design used in the applications of WLAN/WiMAX band, ITU and satellite band system applications.

## References

- Abdel-Rahman, A.B., Verma, A.K., Boutejdar, A. and Omar, A.S. (2004) 'Control of bands top response of Hi-Lo microstrip low pass filter using slot in the ground plane', *IEEE Trans. Microwave Theory Tech.*, Vol. 52, No. 3, pp.1008–1013.
- Abidin, Z.Z., Abd-Alhameed, R.A., McEwan, N.J. and Child, M.B. (2010) 'Analysis of the effect of EBG on the mutual coupling for two-PIFA assembly', *Loughborough Antennas & Propagation Conference*, pp.473–476.
- Alsath, M.G., Kanagasabai, M. and Balasubramanian, B. (2013) 'Implementation of slotted meander line resonators for isolation enhancement in microstrip patch antenna arrays', *IEEE Antennas and Wireless Propagation Letters*, Vol. 12, pp.15–18.
- Bait-Suwailam, M.M., Boybay, M.S. and Ramahi, O.M. (2010) 'Electromagnetic coupling reduction in high-profile monopole antennas using single-negative magnetic metamaterials for MIMO applications', *IEEE Trans. Antennas Propag.*, Vol. 58, No. 9, pp.2894–2902.
- Blanch, S., Romeu, J. and Corbella, I. (2003) 'Exact representation of antenna system diversity performance from input parameter description', *Electron. Letters*, Vol. 39, No. 7, pp.705–707.
- Chae, S.H., Oh, S-K. and Park, S-O. (2007) 'Analysis of mutual coupling, correlations, and TARC in WiBro MIMO array antenna', *IEEE Antennas and Wireless Propagation Letters*, Vol. 6, No. 4, pp.122–125.
- Chaimool, S., Rakuea, C. and Akkarakthalin, P. (2012) 'Compact wideband microstrip thinned array antenna using EBG superstrate', *AEU – International Journal of Electronics and Communications*, Vol. 66, No. 1, pp.49–53.
- Chi, C.Y., Cheng, C.H., Murch, R.D. and Rowell, C.R. (2007) 'Reduction of mutual coupling between closely-packed antenna elements', *IEEE Transactions on Antennas and Propagation*, Vol. 55, No. 6, pp.2341–2349.
- Farsi, S., Schreurs, D. and Nauwelaers, B. (2012) 'Mutual coupling reduction of planar antenna by using a simple microstrip u-section', *IEEE Antennas and Wireless Propagation Letters*, Vol. 11, pp.1501–1503.
- Garg, R., Bahl, I. and Bozzi, M. (2013) 'Defected ground structure (DGS)', in *Microstrip Lines and Slotted Lines*, pp.305–341, Artech House.
- Guha, D., Biswas, M. and Antar, Y.M.M. (2005) 'Microstrip patch antenna with defected ground structure for cross polarization suppression', *IEEE Antennas and Wireless Propagation Letters*, Vol. 4, pp.455–458.
- Islam, M.T. and Alam, M.S. (2013) 'Compact EBG structure for alleviating mutual coupling between patch antenna array elements', *Progress in Electromagnetics Research*, Vol. 137, pp.425–438.
- Khandelwal, M.K., Kanaujia, B.K., Dwari, S., Kumar, S. and Gautam, A.K. (2014a) 'Analysis and design of wide band microstrip line fed antenna with defected ground structure for Ku band applications', *AEU – International Journal of Electronics and Communications*, Vol. 68, No. 10, pp.951–957.
- Khandelwal, M.K., Kanaujia, B.K., Dwari, S., Kumar, S. and Gautam, A.K. (2014b) 'Bandwidth enhancement and cross-polarization suppression in ultra wideband microstrip antenna with defected ground plane', *Microwave and Optical Technology Letters*, Vol. 56, No. 9, pp.2141–2146.
- Kumar, C. and Guha, D. (2012) 'Nature of cross-polarized radiations from probe-fed circular microstrip antennas and their suppression using different geometries of defected ground structure (DGS)', *IEEE Transactions on Antennas and Propagation*, Vol. 60, No. 1, pp.92–101.
- Kumar, C. and Guha, D. (2014) 'Defected ground structure (DGS) – integrated rectangular microstrip patch for improved polarization purity with wide impedance bandwidth', *IET Microwaves, Antennas and Propagation*, Vol. 8, No. 8, pp.589–596.
- Mahmoudian, A. and Rashed-Mohassel, J. (2008) 'Reduction of EMI and mutual coupling in array antennas by using DGS and AMC structures', *PIERS Proceedings*, Hangzhou, China, Vol. 35, pp.106–110.
- Park, S., Kim, C.S., Kim, J., Ahn, D., Qian, J.Y. and Itoh, T. (2001) 'A design of the low-pass filter using the novel microstrip defected ground structure', *IEEE Trans. Microwave Theory Tech.*, Vol. 49, No. 1, pp.86–93.
- Salehi, M. and Tavakoli, A. (2006) 'A novel low mutual coupling microstrip antenna array design using defected ground structure', *AEU – International Journal of Electronics and Communications*, Vol. 60, No. 10, pp.718–723.
- Shafique, M.F., Qamar, Z., Riaz, L., Saleem, R. and Khan, S.A. (2015) 'Coupling suppression in densely packed microstrip arrays using metamaterial structure', *Microwave and Optical Technology Letters*, Vol. 57, No. 3, pp.759–763.
- Shin, H. and Lee, J.H. (2003) 'Capacity of multiple-antenna fading channels: spatial fading correlation, double scattering, and keyhole', *IEEE Trans. Inform. Theory*, Vol. 49, No. 8, pp.2636–2647.
- Stutzman, W.L. and Thiele, G.A. (1998) *Antenna Theory and Design*, 2nd ed., Wiley, New York.
- Sung, Y.J. and Kim, Y.S. (2005) 'An improved design of microstrip patch antennas using photonic bandgap structure', *IEEE Transactions on Antennas and Propagation*, Vol. 53, No. 5, pp.1799–1803.
- Sung, Y.J., Kim, M. and Kim, Y.S. (2003) 'Harmonics reduction with defected ground structure for a microstrip patch antenna', *IEEE Antennas and Wireless Propagation Letters*, Vol. 2, No. 1, pp.111–113.

- Suwailam, M.M.B., Siddiqui, O.F. and Ramahi, O.M. (2010) ‘Mutual coupling reduction between microstrip patch antennas using slotted-complementary split-ring resonators’, *IEEE Antennas Wireless Propagation Letters*, Vol. 9, pp.876–878.
- Xiao, S., Tang, M.C., Bai, Y.Y., Gao, S. and Wang, B.Z. (2011) ‘Mutual coupling suppression in microstrip array using defected ground structure’, *IET Microwaves, Antennas & Propagation*, Vol. 5, No. 12, pp.1488–1494.
- Yang, X.M., Liu, X.G., Zhu, X.Y. and Cui, T.J. (2012) ‘Reduction of mutual coupling between closely packed patch antenna using waveguide meta materials’, *IEEE Antennas and Wireless Propagation Letters*, Vol. 11, pp.389–391.
- Yu, A. and Zhang, X. (2003) ‘A novel method to improve the performance of microstrip antenna arrays using a dumbbell EBG structure’, *IEEE Antennas Wireless Propagation Letters*, Vol. 2, No. 1, pp.170–172.
- Zhu, F.G., Xu, J.D. and Xu, Q. (2009) ‘Reduction of mutual coupling between closely packed antenna elements using defected ground structure’, *Electronic Letters*, Vol. 45, pp.601–602.
- Zulkifli, F.Y., Rahardjo, E.T. and Hartanto, D. (2008) ‘Radiation properties enhancement of triangular patch microstrip antenna array using hexagonal defected ground structure’, *Progress in Electromagnetics Research*, Vol. 5, pp.101–109.
- Zulkifli, F.Y., Rahardjo, E.T. and Hartanto, D. (2010) ‘Mutual coupling reduction using dumbbell defected ground structure for multiband microstrip antenna array’, *Progress in Electromagnetics Research Letters*, Vol. 13, pp.29–40.